ACS OMEGA

http://pubs.acs.org/journal/acsodf

Article

Sterilization Methods and Their Influence on Physicochemical Properties and Bioprinting of Alginate as a Bioink Component

Thomas Lorson,[‖] Matthias Ruopp,[‖] Ali Nadernezhad, Julia Eiber, Ulrich Vogel, Tomasz Jungst, and Tessa Lühmann*

Cite This: *ACS Omega* 2020, 5, 6481−6486

Read Online

ACCESS | Metrics & More | Article Recommendations | Supporting Information

ABSTRACT: Bioprinting has emerged as a valuable three-dimensional (3D) biomanufacturing method to fabricate complex hierarchical cell-containing constructs. Spanning from basic research to clinical translation, sterile starting materials are crucial. In this study, we present pharmacopeia compendial sterilization methods for the commonly used bioink component alginate. Autoclaving (sterilization in saturated steam) and sterile filtration followed by lyophilization as well as the pharmacopeia non-compendial method, ultraviolet (UV)-irradiation for disinfection, were assessed. The impact of the sterilization methods and their effects on physicochemical and rheological properties, bioprinting outcome, and sterilization efficiency of alginate were detailed. Only sterile filtration followed by lyophilization as the sterilization method retained alginate's physicochemical properties and bioprinting behavior while resulting in a sterile outcome. This set of methods provides a blueprint for the analysis of sterilization effects on the rheological and physicochemical pattern of bioink components and is easily adjustable for other polymers used in the field of biofabrication in the future.

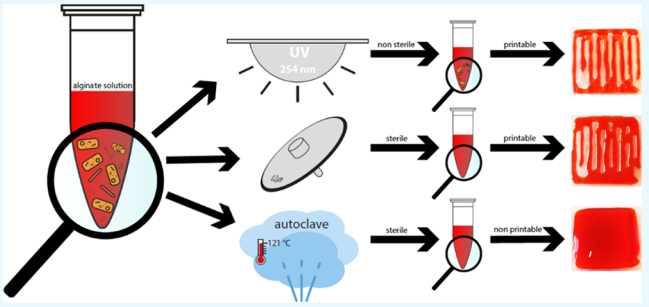

INTRODUCTION

Biofabrication has emerged as a new and rapidly growing field[1] with applications in tissue engineering and regenerative medicine.[2] Generally, biofabrication aims at the generation of hierarchical three-dimensional (3D) and cell-laden scaffolds deploying additive manufacturing.[3] The systematic combination of polymer—either of synthetic[4,5] or natural origin—cells,[6,7] and growth factors leads to so-called bioinks that must fulfill certain characteristics to be taken into consideration for application in a challenging biological environment.[1] The reader is directed to excellent review articles on recent developments in the field of biofabrication.[8−11]

For successfully bridging the gap from research to applied clinical practice, reliable and effective sterilization of the applied polymers is critical during early-stage bioink development.[12] Treatment with 70% ethanol has been suggested as a method for disinfection in biofabrication.[12] However, as a noncompendial method, it is only of limited use for potential clinical translation. Sterility of biomaterials and implants is mandatory, as sadly documented by implant-related infections related to increased patient morbidity and fatalities.[13,14] Sterilization methods include ISO norms (ISO 11737: Sterilization of medical devices) or sterilization monographs described in different pharmacopeias (USP, EP, BP, JP). However, due to the requirements of bioinks, sterilization processes for medical devices (ISO norm) or small molecules and pharmaceutical relevant polymers in solution (pharmacopeial methods) cannot be directly transferred. One reason is the temperature stability, which is in general higher for metals used for load-bearing implants than for polymers as used in bioinks, causing degradation or chemical changes. Consequently, it is important to evaluate the suitability of the sterilization method in line with the physicochemical and mechanical properties of the sterilized material. Although the number of publications dealing with biofabrication has been significantly increasing over the last few years, to the best of our knowledge, only one study investigated sterility and its influence on material properties.[15] In this study, the authors evaluated three sterilization methods on four frequently used biopolymers and identified ethylene oxide (EO) treatment as the most promising one. However, this method is not practicable in every laboratory due to its high safety requirements and high-cost involvement.[16] Furthermore, EO is challenged in light of the clean air act and under review by Food and Drug Administration's (FDA) Environmental Protection Agency (EPA).[17]

Here, we focus on pharmacopeia compendial, potentially high throughput, and cost-effective sterilization methods applicable

Received: December 2, 2019
Accepted: February 20, 2020
Published: March 17, 2020

https://dx.doi.org/10.1021/acsomega.9b04096
ACS Omega 2020, 5, 6481−6486

in routine laboratory work. To this end, we selected sodium alginate as the bioink component, a commonly used bioink in 3D bioprinting, and compared the effects of the sterilization treatment on physicochemical and rheological properties, bioprinting, and sterilization efficiency.

RESULTS AND DISCUSSION

Two compendial sterilization methods, autoclaving (powder and liquid) and sterile filtration, were compared for their sterilization outcome on the polysaccharide alginate (Table 1). For comparison, disinfection with ultraviolet (UV)-light was selected as the noncompendial method.

Table 1. Overview of the Sterilization and Disinfection Methods, Abbreviations, and Their Specifications

name	method	refs
UV-light irradiation (UV)	irradiation with UV-C at 254 nm	18, 19
sterile filtration (filt. + lyo.)	filtration (≤0.22 μm membrane)	20
autoclaving (solution; autoclaved) (powder; autoclaved p.)	sterilization in saturated steam at 121 °C for 15 min	20

First, we analyzed the molar mass distribution of alginate by gel permeation chromatography (GPC) measurements in an aqueous environment after the sterilization or disinfection process (Figure 1A,B). Compared to the nonsterilized alginate polymer, a low molecular tailing at larger retention volumes (5−7 mL) was detected in the RI signal after the autoclaving process (Figure 1A). This finding was corroborated by differential pressure changes, which were lower for autoclaved samples (Figure 2B). Moreover, the resulting number average molar mass (M_n) was statistically significantly lower by 17 and 19 kDa for autoclaved alginate as a powder or in an aqueous solution, respectively (Figure 2C). The weight average molar mass (M_w) was found to be statistically significantly lower after autoclaving alginate as an aqueous solution. The M_w dropped from 77 (±5.2) kDa for native alginate to 53 (±5.6) kDa for the autoclaved alginate. Consequently, dispersity ($Đ$) was only affected by autoclaving alginate as powder, which resulted in a value of around 2.0 (±0.03) and a broader, more heterogenic mass distribution (Figure 2D). These findings corroborate the observations for gelatin and gelatin methacrylate reported by O'Connell et al.[15]

To investigate if the observed changes in the molar mass distribution lead to macroscopic effects on printability, in-depth rheology studies were performed. Oscillatory (Figure 2A,B), as well as rotatory measurements (Figure 2C,D), revealed a distinct impact on material properties. Considerably lower values for the storage (G') and loss modulus (G'') were found for autoclaved samples compared to UV-treated and filtered solutions in the performed amplitude sweep (Figure 2A). We hypothesize that the short-chain fragments that were generated during moist-heat treatment by autoclaving act as a plasticizer, resulting in a reduced chain entanglement of the polymer. Consequently, both the stiffness as well as the energy stored during deformation were reduced, thereby at least in part influencing the printability of alginate. Importantly, all alginate solutions used in the present study did not form gels at 8% (w/v), as demonstrated by $G'' > G'$ notwithstanding the sterilization method. The performed

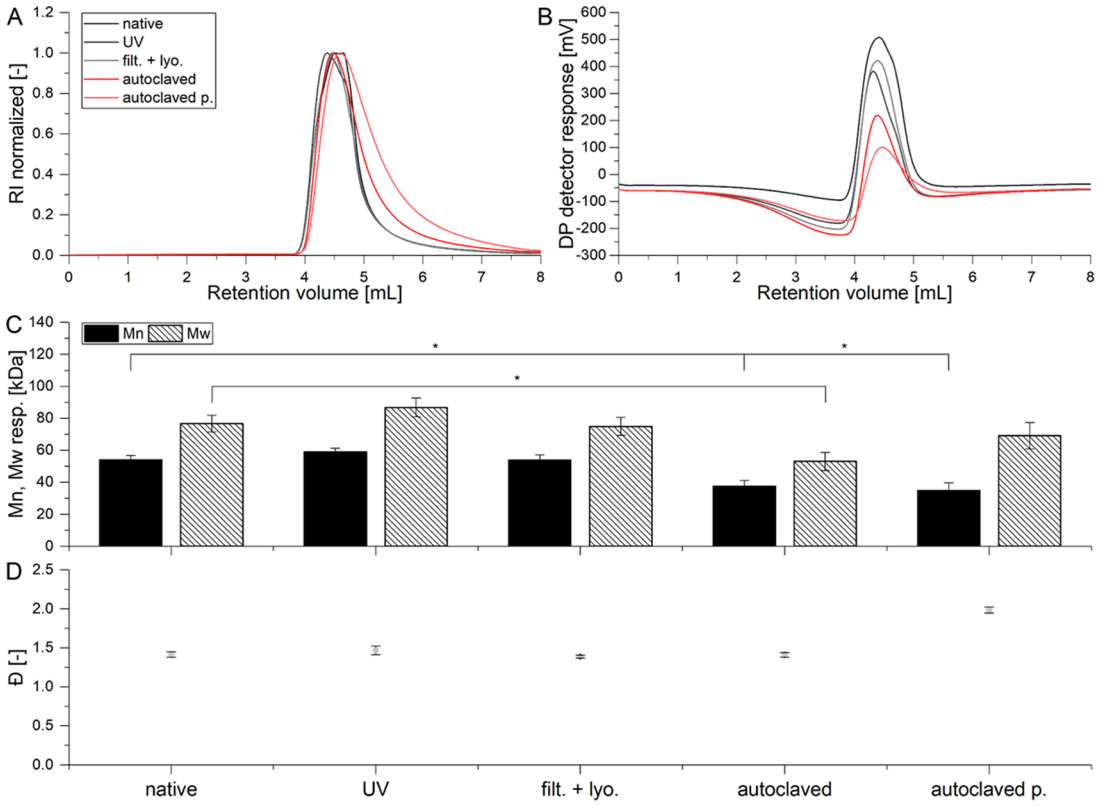

Figure 1. (A) Normalized refractive index and (B) differential pressure detector response signal obtained via GPC at 35 °C using 0.05 M phosphate-buffered saline (PBS) at pH 6.8 as eluent. (C) Calculated M_n, M_w, and (D) $Đ$ values based on calibration with bovine serum albumin. Analysis of variance (ANOVA) was performed, and samples with a p-value <0.05 were considered as statistically significant and are marked with an asterisk (*).

https://dx.doi.org/10.1021/acsomega.9b04096
ACS Omega 2020, 5, 6481−6486

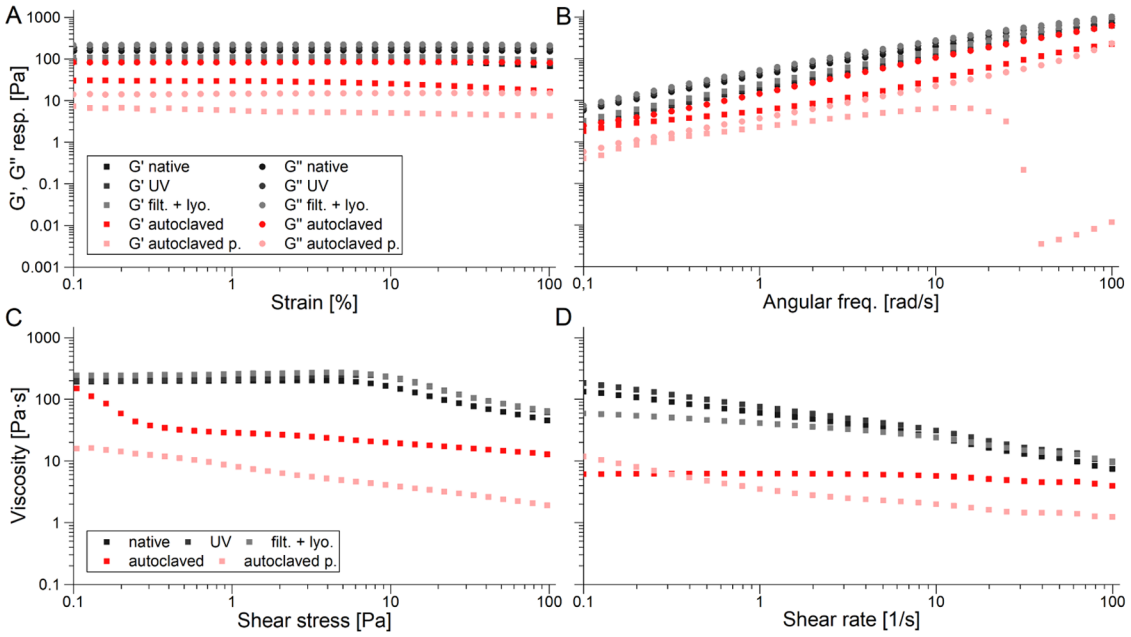

Figure 2. Rheological investigations of aqueous alginate solutions 8% (w/v) at 25 °C. (A) Amplitude sweep from 0.1 to 100% with a constant angular frequency of 10 rad/s. (B) Frequency sweep from 0.1 to 100 rad/s with a constant amplitude of 1%. (C) Shear stress sweep and (D) shear rate sweep from 0.1 to 100 Pa and 0.1 and 100 s^{-1}.

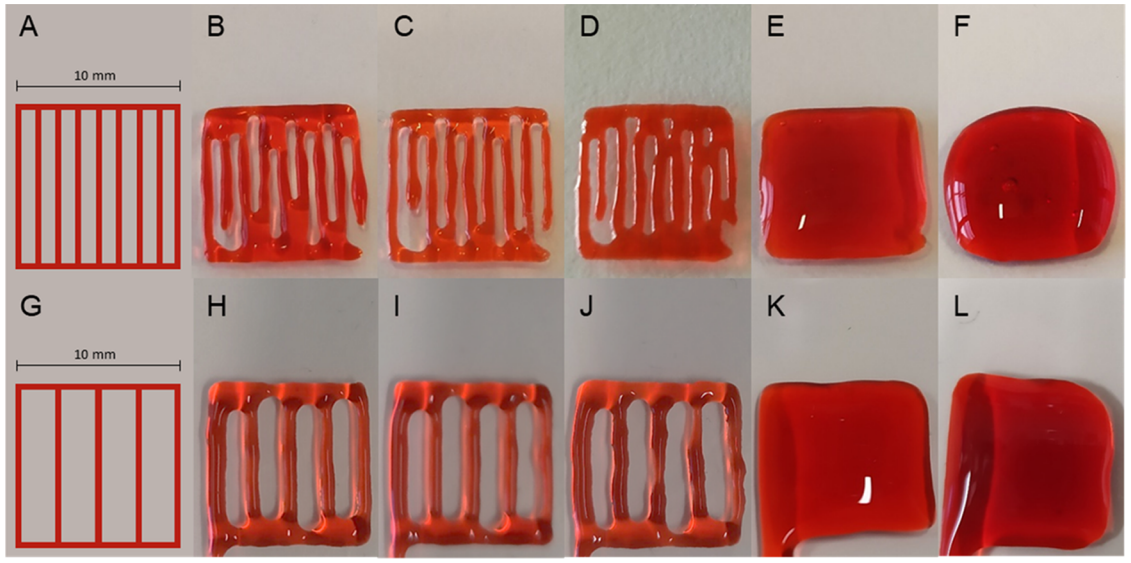

Figure 3. Three-dimension (3D) printed line patterns after different sterilization techniques compared to untreated alginate. (A–F) represents a nine-line pattern and (G–H) a five-line pattern. (A, G) Preset model (B, H) native, (C, I) UV, (D, J) sterile-filtered + lyophilized, (E, K) autoclaved as a solution and (F, L) autoclaved as powder. Printing was performed on a BioX printer (CELLINK, Gothenburg, Sweden) at 25 °C and 120 kPa air pressure. Solutions were stained with Sicopharm Cochineal Red (BASF, Ludwigshafen, Germany) for better contrast.

frequency sweeps confirmed the results and revealed an unexpected rheological behavior for the alginate autoclaved as a powder at frequencies above 10 rad/s (Figure 2B). The elastic component of the alginate material was found to collapse by the order of 4–5 magnitudes with respect to the last value of the linear region (~10 rad/s). This finding was reproduced with additional samples of autoclaved alginate as a powder (n = 3). We assume that the breakdown of elastic components is related to significant degradation of the material during the sterilization process. Moreover, autoclaving caused the disappearance of an explicit yield point present in other samples at around 10 Pa (Figure 2C). Increasing the shear rate from 0.1 to 100 s^{-1} revealed shear thinning from 132.9 (±33.6) to 2.8 (±0.1) Pa·s for untreated, from 183.7 (±56.8) to 3.7 (± 0.4) Pa·s for UV-irradiated samples, and from 59.1 (±8.6) to 3.9 (±0.3) Pa·s for sterile-filtered samples (Figure 2D). This rheological behavior is typically observed for polymer solutions due to the increasing orientation of the polymer chains with an increasing shear rate.[4,7] The viscosity was significantly lower for autoclaved samples and only a minor shear-thinning effect due to the amount of low molecular chain fragments was observed. The viscosity decreased from 6.1 (±0.9) to 2.2 (±0.1) Pa·s for alginate autoclaved as an aqueous solution and from 11.8 (±4.5) to 0.9 (± 0.1) Pa·s for alginate autoclaved as powder.

https://dx.doi.org/10.1021/acsomega.9b04096
ACS Omega 2020, 5, 6481–6486

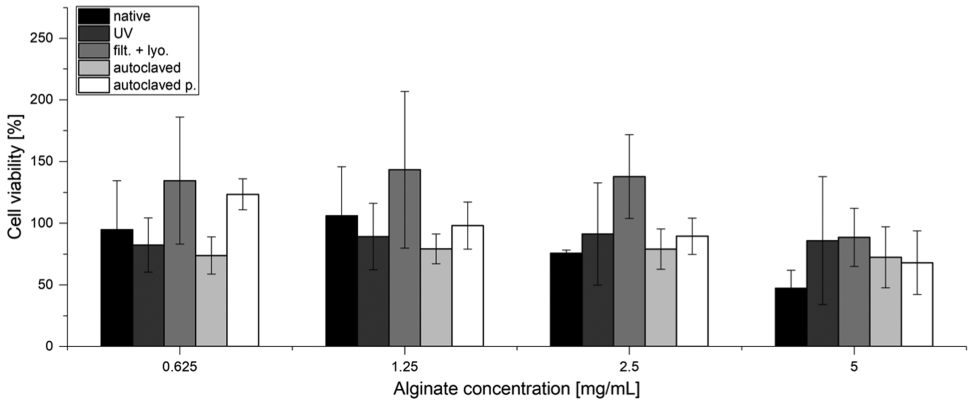

Figure 4. Cell viability was examined via WST-1 cell proliferation assay at 450 and 630 nm with increasing alginate concentrations (mean ± standard deviation, n = 3). Measurements were performed after 24 h of incubation at 37 °C and 5% CO_2. ANOVA was not significant among tested concentrations of alginates (p-value <0.05).

To this end, we used 3D printing experiments to analyze if the observed changes impact the rheology of the autoclaved alginate solutions and hence their printability (Figure 3). Therefore, line patterns were used as a default for the 3D printing process (Figure 3A,G).[21−24] Two different distances between the lines were used to determine whether a larger distance has a positive effect on the printability of the autoclaved alginate solutions. After printing, the autoclaved solutions, independent of whether autoclaved as powder or solution, revealed a loss of their shape fidelity (Figure 3E,F,K,L). In these autoclaved solutions, extrusion leads to wide viscous strands, which immediately merged into each other resulting in a fully filled construct. The shape-loss effect was more pronounced with alginate that was autoclaved as a powder (Supporting Videos S4, S5, S9, and S10). These findings are supported by the changes in the rheological behavior and reduced molecular weight (Figures 1C and 2) discussed previously. In contrast, printed line structures for all other alginates (native, UV-irradiated, and sterile-filtered samples) were preserved and retained their shape. Native, UV-treated, and sterile-filtered alginate solutions were printable with accuracy tradeoffs at the points where the printer positioned the needle for the extrusion of new lines. Moreover, all samples revealed a slight interlacing of the lines at the turning points of the given line structure. This finding may be attributed to the absence of $CaCl_2$ for stabilization of the 3D printed structure by alginate cross-linking.[25] As cross-linking is time- and concentration-dependent and furthermore depends on the available surface in contact with the cross-linking agent, the addition of $CaCl_2$ was avoided to allow direct comparison of the printing outcome without postprinting modification.

Sodium alginate, approved by the FDA[26] as a food-additive, is considered as noncytotoxic.[27] To investigate if degradation products formed during the sterilization process of alginate influence cell viability, the metabolic activity of NIH 3T3 cells was monitored deploying WST-1 proliferation assay with increasing alginate concentrations (Figure 4). It is important to note that no gel formation occurred due to the use of calcium-free Dulbecco's modified Eagle's medium (DMEM). No significant differences between the differently sterilized alginates were observed, indicating good cell compatibility of all alginates after the sterilization process. Important to note is that only the influence of the material was investigated while bioprinting was not investigated.

In a final step, we evaluated the sterility of all samples discussed above according to the European Pharmacopeia. Beforehand, the inhibitory effects of all polymer samples were excluded by validation with various type of strains prescribed in the European Pharmacopeia. Sterility testing revealed the existence of *Bordetella bronchiseptica* in the unsterilized starting material and in the UV-treated alginate sample (Figure S1). In contrast, the sterile-filtered and subsequently lyophilized alginate sample remained sterile after 14 days of incubation in liquid media. These findings are of major importance as disinfection by UV-light is frequently used in the field of biofabrication.

CONCLUSIONS

By analyzing pharmacopeia compendial methods for sterilization of the model bioink component alginate, we developed sterilization strategies suitable for sensitive polymers applied in biofabrication. First, sterilization of a potential bioink should be investigated in the early phase of bioink development. Second, UV-light treatment as a noncompendial method was not effective in terms of sterilization outcomes and should be avoided. Based on the examined methods, we recommend sterile filtration at low polymer concentrations followed by lyophilization to obtain both sterile and printable bioinks.

MATERIALS AND METHODS

Sodium Alginate Solutions. Sodium alginate (Protanal LF 10/60 FT) was obtained from FMC BioPolymer (Philadelphia, PA). Sodium chloride (NaCl), monobasic sodium phosphate (NaH_2PO_4), and dibasic sodium phosphate (Na_2HPO_4) were purchased from Sigma-Aldrich (Steinheim, Germany) and were used without further purification. The lyophilized powders were stored at −20 °C prior to use.

Sodium alginate solution was prepared by dissolving sodium alginate powder either native or sterilized in MilliQ water for 24 h at 35 °C and 600 rpm in a Thermomixer comfort (Eppendorf, Wesseling-Berzdorf, Germany).

Cell Culture Material. Dulbecco's modified Eagle's medium (DMEM; high glucose, no calcium, no glutamine; catalog no. 21068028), fetal bovine serum (FBS; ref 10270-106), and Nunc 96-well plates were purchased from Thermo Fisher Scientific (Schwerte, Germany). Penicillin G and streptomycin solutions were purchased from Biochrom AG (Berlin, Germany). Water-soluble tetrazolium salt 1 (WST-1) was purchased from Roche (Basel, Switzerland).

https://dx.doi.org/10.1021/acsomega.9b04096
ACS Omega 2020, 5, 6481−6486

Sterilization. Autoclave sterilization of sodium alginate was performed in a DX-90 2D autoclave (Systec, Linden, Germany) according to the European Pharmacopoeia for 15 min at 121 °C for solutions and powders. Sterile filtration was performed by filtering the sodium alginate solution (1%, w/v) through a Filtropur S 0.2 μm polyethersulfone (PES) syringe filter (Sarstedt, Nümbrecht, Germany) under a Safe 2020 clean bench (Fisher Scientific, Schwerte, Germany). The filtered samples were then frozen at −80 °C and lyophilized in syringes equipped with a Filtropur S 0.2 μm syringe filter for 48 h at 11 μbar. UV-light sterilization of sodium alginate powder was performed under a TL-900 universal UV lamp (Camag, Muttenz, Switzerland) at 254 nm wavelength and a distance of 2 cm for 1 h.

Sterility Testing. Sterility testing was conducted at the Institute for Hygiene and Microbiology of the University of Würzburg using the Steritest Symbio pump (Merck, Darmstadt, Germany). The laboratory is accredited according to the standard DIN EN ISO 17025. Specimen handling and filtration were conducted under a safety cabinet in a clean room. The product solutions (4−9 mL) were filtered according to the manufacturer's instructions. The system splits the sample into two parts for separate incubation in thioglycollate broth and soybean−casein digest medium. Following rinsing with fluid A (Merck, Darmstadt, Germany), the samples were incubated in soybean−casein digest medium and thioglycollate broth at 23 and 33 °C, respectively, for 14 days. They were visually inspected for turbidity every working day. In case of possible bacterial growth, 0.5 mL of the liquid medium was inoculated each on chocolate agar (Becton Dickinson, Franklin Lakes, USA), Schaedler agar with vitamin K1 and 5% sheep blood (Becton Dickinson, Franklin Lakes, USA), and Sabouraud agar with penicillin and streptomycin (Becton Dickinson, Franklin Lakes, USA). The agar plates were incubated at 23 or 33 °C for up to 5 days. In the case of Schaedler agar, incubation took place in an anaerobic atmosphere. In the case of growth, colonies according to their morphology were isolated and subjected to Vitek mass spectrometry (MS) analysis for bacterial species assignment. Validation by assessment of possible microbial growth inhibition by the product was conducted using *Staphylococcus aureus* (ATCC 6538), *Clostridium sporogenes* (ATCC 19404), and *Pseudomonas aeruginosa* (ATCC 9027) for thioglycollate broth and *Aspergillus brasiliensis* (ATCC 16404), *Candida albicans* (ATCC 10231), and *Bacillus subtilis* (ATCC 6633) for soybean−casein digest medium. In none of the strains, a negative impact of the product on microorganism recovery was observed.

Rheology. Rheological experiments were performed on the system described below.

A Physica MCR 302 rheometer (Anton Paar, Graz, Austria) equipped with a heating mantle (H-PTD 200) and plate−plate geometry (PP25 measuring plate) was utilized. Data were processed using RheoCompass software version 1.23.378 (Anton Paar, Graz, Austria).

Gel Permeation Chromatography (GPC). All GPC measurements were performed on a Malvern Viscotek GPCmax system with an integrated isocratic pump, autosampler, and a Viscotek 305 TDA triple detector (Malvern Panalytical, Kassel, Germany). A Phenomenex BioSep SEC-s4000 and SEC-s2000 column in series with 5 μm particle size and 145 Å pore size (4.6 × 300 mm^2), and a guard column at 298 K and 0.05 M PBS at a pH of 6.8 were used. The flow rate was adjusted to 0.3 mL/min. Prior to each measurement, the samples were filtered through a Whatman Puradisc 0.2 μm PES syringe filter (GE Healthcare, Chicago) to remove particles. Data were processed using OmniSEC software version 5.12 (Malvern Panalytical, Kassel, Germany).

Cytotoxicity. NIH 3T3 fibroblasts were seeded in a microplate at a concentration of 2000 cells per well in calcium-free DMEM and incubated overnight at 37 °C and 5% CO_2. The following day, 80 mg/mL stock solutions of alginate in MilliQ water, treated with different sterilization techniques, were diluted with calcium-free DMEM to 10, 5, 2.5, and 1.25 mg/mL and added 1:1 to the fibroblasts in triplicates resulting in final alginate concentrations of 5, 2.5, 1.25, and 0.625 mg/mL, respectively. After 24 h of incubation at 37 °C and 5% CO_2, the solutions were aspirated and the cells were washed twice with PBS. Afterward, each well was treated with a mixture of 10 parts DMEM and one part WST-1. Then the absorbance was measured at 450 nm (soluble formazan product) and 630 nm (background noise) with a Spectramax 250 microplate reader (Molecular Devices, San José, USA).

Statistical Analysis. For statistical analysis, analysis of variance (ANOVA) was performed with OriginPro 2017 (OriginLab Corporation, Northampton, USA). Samples with a p-value <0.05 were considered as statistically significant and are marked with an asterisk (*).

■ ASSOCIATED CONTENT

Supporting Information

The Supporting Information is available free of charge at https://pubs.acs.org/doi/10.1021/acsomega.9b04096.

3D bioprinting process of the native alginate solution in a 9 line pattern (MP4)

3D bioprinting process of the UV irradiated alginate solution in a 9 line pattern (MP4)

3D bioprinting process of the sterile filtered and lyophilized alginate solution in a 9 line pattern (MP4)

3D bioprinting process of the autoclaved alginate solution in a 9 line pattern (MP4)

3D bioprinting process of the alginate solution autoclaved as powder in a 9 line pattern (MP4)

3D bioprinting process of the native alginate solution in a 5 line pattern (MP4)

3D bioprinting process of the UV irradiated alginate solution in a 5 line pattern (MP4)

Sterile sample (left), sample containing *B. bronchiseptica* (middle), and test bacterium (*S. aureus*, right) in soy casein pepton (PDF)

3D bioprinting process of the sterile filtered and lyophilized alginate solution in a 5 line pattern (MP4)

3D bioprinting process of the autoclaved alginate solution in a 5 line pattern (MP4)

3D bioprinting process of the alginate solution autoclaved as powder in a 5 line pattern (MP4)

■ AUTHOR INFORMATION

Corresponding Author

Tessa Lühmann − *Institute of Pharmacy and Food Chemistry, University of Würzburg, 97074 Würzburg, Germany*; Phone: +49 931 318 28 07; Email: tessa.luehmann@.uni-wuerzburg.de; Fax: +49 931 318 46 08

https://dx.doi.org/10.1021/acsomega.9b04096
ACS Omega 2020, 5, 6481−6486

Authors

Thomas Lorson − *Institute of Pharmacy and Food Chemistry, University of Würzburg, 97074 Würzburg, Germany*

Matthias Ruopp − *Institute of Pharmacy and Food Chemistry, University of Würzburg, 97074 Würzburg, Germany*

Ali Nadernezhad − *Department of Functional Materials in Medicine and Dentistry and Bavarian Polymer Institute, Universitätsklinikum Würzburg, 97070 Würzburg, Germany*

Julia Eiber − *Institute of Pharmacy and Food Chemistry, University of Würzburg, 97074 Würzburg, Germany*

Ulrich Vogel − *Institut für Hygiene und Mikrobiologie, Universitätsklinikum Würzburg, 97080 Würzburg, Germany*

Tomasz Jungst − *Department of Functional Materials in Medicine and Dentistry and Bavarian Polymer Institute, Universitätsklinikum Würzburg, 97070 Würzburg, Germany*

Complete contact information is available at: https://pubs.acs.org/10.1021/acsomega.9b04096

Author Contributions

[‖]T.L. and M.R. contributed equally to this work.

Notes

The authors declare no competing financial interest.

■ ACKNOWLEDGMENTS

The authors gratefully acknowledge financial support by the German Federal Ministry of Education and Research BMBF (FKZ 13XP5071D) and of the German Research Foundation (DFG) within the collaborative research center SFB TRR225 (subproject A03). The expert technical assistance of Sandra Büchner is gratefully acknowledged. This publication was supported by the Open Access Publication Fund of the University of Wuerzburg.

■ REFERENCES

(1) Groll, J.; Burdick, J. A.; Cho, D. W.; Derby, B.; Gelinsky, M.; Heilshorn, S. C.; Jungst, T.; Malda, J.; Mironov, V. A.; Nakayama, K.; Ovsianikov, A.; Sun, W.; Takeuchi, S.; Yoo, J. J.; Woodfield, T. B. F. A definition of bioinks and their distinction from biomaterial inks. *Biofabrication* **2018**, *11*, No. 013001.

(2) Murphy, S. V.; Atala, A. 3D Bioprinting of tissues and organs. *Nat. Biotechnol.* **2014**, *32*, 773−785.

(3) Malda, J.; Visser, J.; Melchels, F. P.; Jungst, T.; Hennink, W. E.; Dhert, W. J.; Groll, J.; Hutmacher, D. W. 25th anniversary article: Engineering hydrogels for Biofabrication. *Adv. Mater.* **2013**, *25*, 5011−5028.

(4) Lorson, T.; Jaksch, S.; Lubtow, M. M.; Jungst, T.; Groll, J.; Luhmann, T.; Luxenhofer, R. A Thermogelling Supramolecular Hydrogel with Sponge-Like Morphology as a Cytocompatible bioink. *Biomacromolecules* **2017**, *18*, 2161−2171.

(5) Müller, M.; Becher, J.; Schnabelrauch, M.; Zenobi-Wong, M. Nanostructured Pluronic hydrogels as bioinks for 3D Bioprinting. *Biofabrication* **2015**, *7*, No. 035006.

(6) Bertlein, S.; Brown, G.; Lim, K. S.; Jungst, T.; Boeck, T.; Blunk, T.; Tessmar, J.; Hooper, G. J.; Woodfield, T. B. F.; Groll, J. Thiol-Ene Clickable Gelatin: A Platform bioink for Multiple 3D Biofabrication Technologies. *Adv. Mater.* **2017**, *29*, No. 1703404.

(7) Highley, C. B.; Rodell, C. B.; Burdick, J. A. Direct 3D Printing of Shear-Thinning Hydrogels into Self-Healing Hydrogels. *Adv. Mater.* **2015**, *27*, 5075−5079.

(8) Mironov, V.; Trusk, T.; Kasyanov, V.; Little, S.; Swaja, R.; Markwald, R. Biofabrication: a 21st century manufacturing paradigm. *Biofabrication* **2009**, *1*, No. 022001.

(9) Hospodiuk, M.; Dey, M.; Sosnoski, D.; Ozbolat, I. T. The bioink: A comprehensive review on bioprintable materials. *Biotechnol. Adv.* **2017**, *35*, 217−239.

(10) Gopinathan, J.; Noh, I. Recent trends in bioinks for 3D printing. *Biomater. Res.* **2018**, *22*, No. 11.

(11) Gungor-Ozkerim, P. S.; Inci, I.; Zhang, Y. S.; Khademhosseini, A.; Dokmeci, M. R. bioinks for 3D Bioprinting: an overview. *Biomater. Sci.* **2018**, *6*, 915−946.

(12) Rutz, A. L.; Lewis, P. L.; Shah, R. N. Toward next-generation bioinks: Tuning material properties pre- and post-printing to optimize cell viability. *MRS Bull.* **2017**, *42*, 563−570.

(13) Galante, R.; Pinto, T. J. A.; Colaco, R.; Serro, A. P. Sterilization of hydrogels for biomedical applications: A review. *J. Biomed. Mater. Res., Part B* **2018**, *106*, 2472−2492.

(14) Rutala, W. A.; Weber, D. J. Infection control: the role of disinfection and sterilization. *J. Hosp. Infect.* **1999**, *43*, S43−S55.

(15) O'Connell, C. D.; Onofrillo, C.; Duchi, S.; Li, X.; Zhang, Y.; Tian, P.; Lu, L.; Trengove, A.; Quigley, A.; Gambhir, S.; Khansari, A.; Mladenovska, T.; O'Connor, A.; Di Bella, C.; Choong, P. F.; Wallace, G. G. Evaluation of sterilisation methods for bio-ink components: gelatin, gelatin methacryloyl, hyaluronic acid and hyaluronic acid methacryloyl. *Biofabrication* **2019**, *11*, No. 035003.

(16) Basu, D.; Bag, S.; Das, A.; Rozario, J.; Goel, G. Comparing sterilization efficacy and cost implications of various gas-based sterilization methods used in a Central Sterile Supply Department: A short review. *J. Acad. Clin. Microbiol.* **2018**, *20*, 108.

(17) Ethylene Oxide Sterilization for Medical Devices. https://www.fda.gov/medical-devices/general-hospital-devices-and-supplies/ethylene-oxide-sterilization-medical-devices (accessed Nov 12, 2019).

(18) Gupta, A.; Avci, P.; Dai, T.; Huang, Y. Y.; Hamblin, M. R. Ultraviolet Radiation in Wound Care: Sterilization and Stimulation. *Adv. Wound Care* **2013**, *2*, 422−437.

(19) Lah, E. F. C.; Musa, R. N. A. R.; Ming, H. T. Effect of germicidal UV-C light(254 nm) on eggs and adult of house dustmites, Dermatophagoides pteronyssinus and Dermatophagoides farinae (Astigmata: Pyroglyhidae). *Asian Pac. J. Trop. Biomed.* **2012**, *2*, 679−683.

(20) Methoden zur Herstellung steriler Zubereitungen In *European Pharmacopoeia* 9th ed., 2017, pp 923 925.

(21) Pati, F.; Jang, J.; Ha, D. H.; Won Kim, S.; Rhie, J. W.; Shim, J. H.; Kim, D. H.; Cho, D. W. Printing three-dimensional tissue analogues with decellularized extracellular matrix bioink. *Nat. Commun.* **2014**, *5*, No. 3935.

(22) Paxton, N.; Smolan, W.; Bock, T.; Melchels, F.; Groll, J.; Jungst, T. Proposal to assess printability of bioinks for extrusion-based Bioprinting and evaluation of rheological properties governing bioprintability. *Biofabrication* **2017**, *9*, No. 044107.

(23) Berg, J.; Hiller, T.; Kissner, M. S.; Qazi, T. H.; Duda, G. N.; Hocke, A. C.; Hippenstiel, S.; Elomaa, L.; Weinhart, M.; Fahrenson, C.; Kurreck, J. Optimization of cell-laden bioinks for 3D Bioprinting and efficient infection with influenza A virus. *Sci. Rep.* **2018**, *8*, No. 13877.

(24) Stanton, M. M.; Samitier, J.; Sanchez, S. Bioprinting of 3D hydrogels. *Lab Chip* **2015**, *15*, 3111−3115.

(25) Grant, G. T.; Morris, E. R.; Rees, D. A.; Smith, P. J. C.; Thom, D. Biological interactions between polysaccharides and divalent cations: The egg-box model. *FEBS Lett.* **1973**, *32*, 195−198.

(26) Gao, Y. Z.; Chang, T. X.; Wu, Y. X. In-situ synthesis of acylated sodium alginate-g-(tetrahydrofuran5-b-polyisobutylene) terpolymer/Ag-NPs nanocomposites. *Carbohydr. Polym.* **2019**, *219*, 201−209.

(27) Pawar, S. N.; Edgar, K. J. Alginate derivatization: a review of chemistry, properties and applications. *Biomaterials* **2012**, *33*, 3279−3305.